

Atmospheric emission of nanoplastics from sewer pipe repairs

Received: 14 December 2021

Accepted: 22 August 2022

Published online: 6 October 2022

 Check for updates

Ana C. Morales¹, Jay M. Tomlin¹, Christopher P. West¹, Felipe A. Rivera-Adorno¹, Brianna N. Peterson¹, Steven A. L. Sharpe¹, Yoorae Noh², Seyedeh M. T. Sendesi², Brandon E. Boor², John A. Howarter³, Ryan C. Moffet⁴, Swarup China⁵, Brian T. O'Callahan⁶, Patrick Z. El-Khoury⁵, Andrew J. Whelton^{2,7} and Alexander Laskin¹ ✉

Nanoplastic particles are inadequately characterized environmental pollutants that have adverse effects on aquatic and atmospheric systems, causing detrimental effects to human health through inhalation, ingestion and skin penetration^{1–3}. At present, it is explicitly assumed that environmental nanoplastics (EnvNPs) are weathering fragments of microplastic or larger plastic debris that have been discharged into terrestrial and aquatic environments, while atmospheric EnvNPs are attributed solely to aerosolization by wind and other mechanical forces. However, the sources and emissions of unintended EnvNPs are poorly understood and are therefore largely unaccounted for in various risk assessments⁴. Here we show that large quantities of EnvNPs may be directly emitted into the atmosphere as steam-laden waste components discharged from a technology commonly used to repair sewer pipes in urban areas. A comprehensive chemical analysis of the discharged waste condensate has revealed the abundant presence of insoluble colloids, which after drying form solid organic particles with a composition and viscosity consistent with EnvNPs. We suggest that airborne emissions of EnvNPs from these globally used sewer repair practices may be prevalent in highly populated urban areas⁵, and may have important implications for air quality and toxicological levels that need to be mitigated.

Environmental pollution by the degradation products of plastic materials is an emerging worldwide concern, with the majority of studies focusing on the occurrence, fate and effects of micro- and nanoplastics in marine and terrestrial environments^{6–9}. At present, it is assumed that microplastics enter the environment as a result of the fragmentation of large plastic objects and synthetic textiles through photochemical, biotic and abiotic degradation processes, and by the direct emission of engineered nanometre-to-micrometre size plastic

beads, such as those commonly used in cosmetic products. The continuing degradation of microplastic beads (<5 mm) and fragments results in additional nanoscale plastics (<1 µm), which increases the diversity of environmental nanoplastics (EnvNPs)⁴. EnvNPs are considered a unique class of pollutants that can be distinguished from both microplastics and engineered nanoparticles through their unique physical properties and chemical composition⁴. Because of their very small size and low degradation rate, EnvNPs pose threats to ecosystems^{6,10} and

¹Department of Chemistry, Purdue University, West Lafayette, IN, USA. ²Lyles School of Civil Engineering, Purdue University, West Lafayette, IN, USA.

³School of Materials Engineering, Purdue University, West Lafayette, IN, USA. ⁴Sonoma Technology, Petaluma, CA, USA. ⁵Physical Sciences Division,

Pacific Northwest National Laboratory, Richland, WA, USA. ⁶Environmental Molecular Sciences Laboratory, Pacific Northwest National Laboratory,

Richland, WA, USA. ⁷Department of Environmental and Ecological Engineering, Purdue University, West Lafayette, IN, USA. ✉e-mail: alaskin@purdue.edu

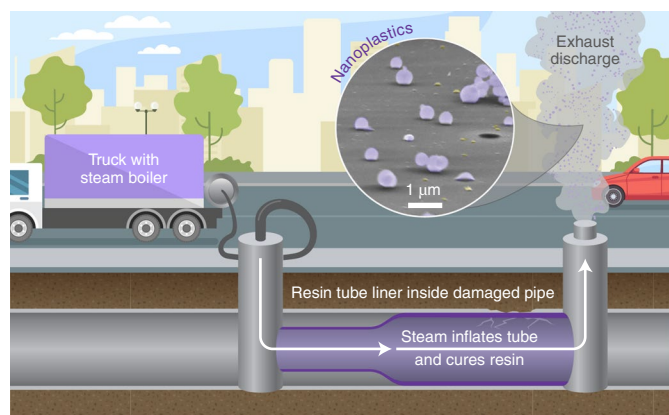


Fig. 1 | A schematic illustration of CIPP installation. A flexible resin-impregnated tube is first inserted into the damaged pipe. This tube is inflated against the damaged pipe wall by pumping ambient air, water and/or steam through the tube. Next, the tube is cured in place using either thermal (hot steam injected into the tube) or ultraviolet curing methods, and the waste is discharged into the environment. After curing, the newly installed plastic pipe is cooled by blowing forced ambient air through the tube, also resulting in the atmospheric discharge of waste laden with EnvNP particles.

are also considered of immediate (acute) toxicological concern as a result of direct inhalation and deposition in lungs⁴. Long-term (chronic) toxicological effects also occur through their bioaccumulation in food chains, which eventually leads to ingestion by humans, posing additional threats to human health^{2,3,11}. Compared with the plethora of studies of microplastics in marine and terrestrial environments, reports on EnvNP particles, especially their airborne occurrences, are scarce. The observations reported here challenge our understanding of EnvNP formation and suggest that common municipal practices of sewer pipe repairs constitute a direct atmospheric emission source.

The cured-in-place-pipe (CIPP) installation of plastic pipes is the most popular, least expensive and most frequently used technology used to cure leaking sanitary and stormwater sewers through the insertion of new plastic pipes inside the existing pipes (Fig. 1)⁵. Waste plumes discharged during CIPP manufacture are complex multiphase mixtures of volatile and semi-volatile organic compounds (VOC and SVOC, respectively), primary and secondary organic aerosols, and the fine debris of partially cured resin, all blown into the atmosphere at substantial concentrations at worksites (Supplementary Video 1). Specifically, detected VOCs are reported^{12–14} to be at the level of 394–757 parts per million by volume, which is four to five orders of magnitude higher than the background VOC concentrations (<100 ppb) reported even in heavily polluted urban areas¹⁵. While dispersion model analysis and field measurements show notable dilution of the VOC concentrations down to sub-parts per million levels at distances of ~50 m downwind, local instances of degraded air quality have affected both indoor and outdoor environments in urban neighbourhoods and even prompted building evacuations^{13,16}. Furthermore, recent field measurements^{16,17} have shown that additional condensed-phase organic pollutants are also emitted into the atmosphere around CIPP installation sites, although their qualitative and quantitative characteristics are as yet largely unknown.

Analysis of the discharged waste condensate collected at four CIPP operation sites (labelled X1, X2, X4 and X5 in Supplementary Note 1) revealed the abundant presence of colloidal material; this colloidal material forms airborne particles as water evaporates from microdroplets of the discharged waste. An array of complementary analytical measurements were used for the systematic characterization of both the colloidal material and the resulting dry particles (Supplementary Note 2). Figure 2 illustrates the particle mass size distributions of both

the wet colloids detected in the condensate samples (Supplementary Note 3) and the aerosolized dry particles generated from the same samples (Supplementary Note 4). In all four samples, the sizes of the wet colloids and dry particles are in the submicrometre range: the mean sizes of the wet colloids and dry particles are ~1 and ~0.5 µm, respectively. The submicrometre particles remain airborne for days to weeks¹⁸, and therefore they need to be viewed as air pollutants emitted at CIPP installation sites. Quantitative assessment of the mass loadings of the condensed-phase organic material emitted as dry aerosol particles per litre of discharged waste condensate revealed values of between 0.01 and 3.24 mg l⁻¹ for the four reported samples (Supplementary Note 4). The highest mass loading of 1.65–3.24 mg l⁻¹ was estimated for the CIPP installation site X1, where the highest concentrations of gas-phase styrene (well-known polymerization component) were evident (Supplementary Table 1). This correlation between high levels of emitted styrene and particulates strongly suggests that the chemical composition of the dry particles is likely to show a close resemblance to the polymeric structure of the nanoplastics. Furthermore, molecular analysis of the solvent-dissolved components of the CIPP condensate from the X1 site showed a very complex mixture of chemical pollutants that can polymerize and partition between gaseous, aqueous and solid phases when water evaporates from the discharged steam-laden waste. Chemical characterization of this mixture using liquid chromatography coupled to photodiode array and high-resolution mass detectors uncovered a wide range of molecular components with a broad variation in molecular weight, structure and degree of oxidation (Supplementary Note 5). Many of the identified compounds were polymer precursors and initiators, plausibly washed out from the surface of the uncured resin tube. Among them are various hazardous air pollutants (phenol, dibutyl phthalate and styrene) controlled by the US Environmental Protection Agency¹⁹, known and suspected carcinogens (styrene, benzo[ghi]perylene and pyrene)²⁰, endocrine-disrupting compounds (dibutyl phthalate and styrene)²¹ and compounds with little toxicity data (bis(4-*tert*-butylcyclohexyl) peroxydicarbonate). The detection of polymer precursors and various low-volatility components in these mixtures prompts the hypothesis that the evaporation of water from microdroplets of discharged waste would result in the solidification of dry particles, and that their chemical composition and physical properties would resemble EnvNPs⁴. A mechanism describing the peroxide-initiated radical polymerization of CIPP monomer styrene is illustrated in Supplementary Scheme 1 in Supplementary Note 6. However, it is also plausible that common environmental aqueous-phase oligomerization reactions^{22–28} (Supplementary Scheme 2) will concurrently occur in the drying microdroplets, producing solid EnvNPs with variable composition.

Consistent with this hypothesis, spectromicroscopic analysis of the chemical composition, viscoelastic properties and internal and external mixing states of the dry particles generated from the waste condensate samples showed that their characteristics are very much consistent with EnvNPs. Figure 3a shows a representative scanning electron microscopy (SEM) image, acquired at a tilt angle of 75°, of dry particles generated from the X1 sample, deposited on an impactor substrate. Upon impact with the substrate, the particles deform and the extent of this deformation is used to estimate their viscosity (Supplementary Note 7). The viscosity estimates shown in Fig. 3b indicate high fractions (40–80%, for the four samples) of solid particles with a viscosity of ≥10¹⁰ Pa s, similar to plastic materials²⁹. Such high viscosity indicates that they originate either from a partial disintegration of the resin tube material or from aqueous-phase polymerization of the soluble components of the waste as the aerosol mist dries out²⁹.

Computer-controlled SEM with energy-dispersed X-ray microanalysis (CCSEM–EDX) performed on over >2,000 particles in each of the four samples showed their predominantly carbonaceous composition, with only minor contributions from inorganic salts or mineral dust (Supplementary Note 9), consistent with the suggested designation

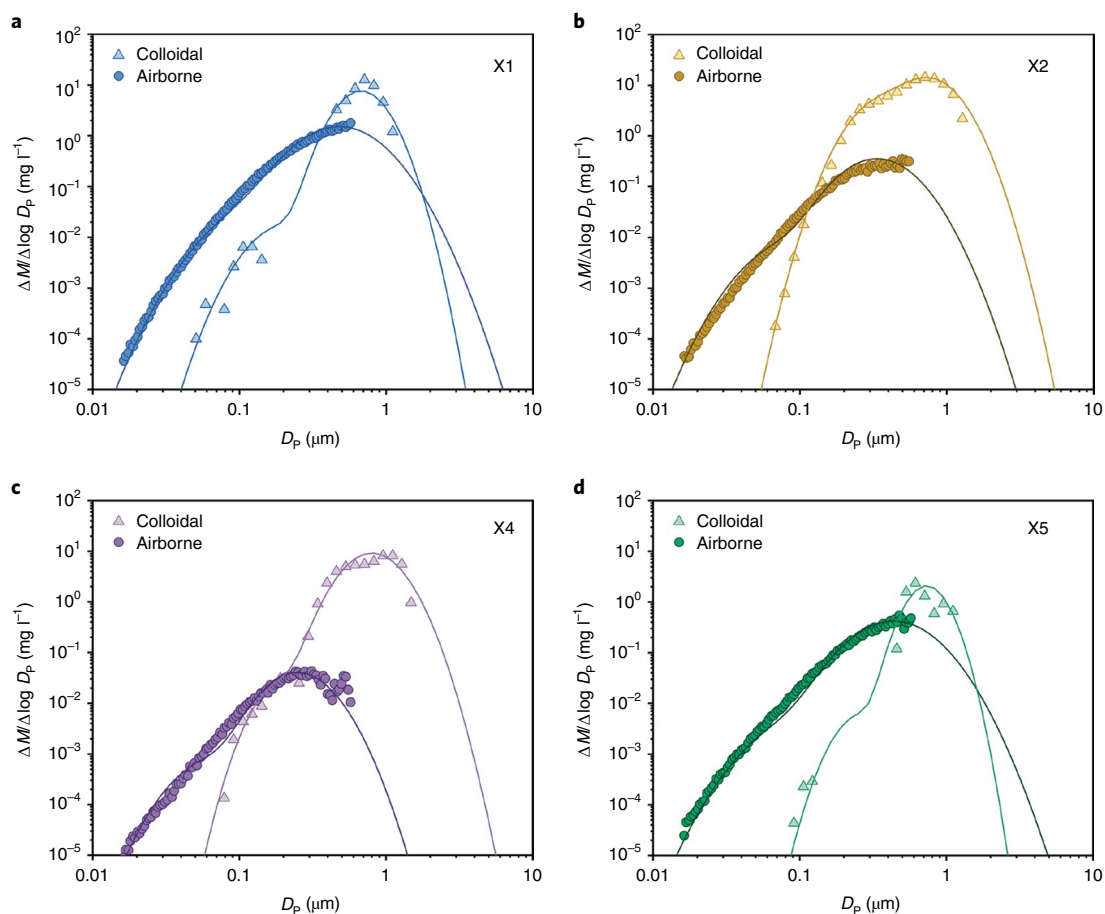


Fig. 2 | Particle mass size distributions of wet colloids and dry particles from CIPP waste. Particle mass size distributions of wet colloids in CIPP waste condensate samples and dry particles aerosolized from the same samples collected at four different operation sites (X1, X2, X4 and X5). The

lines show bimodal lognormal data fits; the fitting parameters are tabulated in Supplementary Table 2. D_p , particle diameter; $\Delta M/\Delta \log D_p$, mass concentration. The mass concentration values are reported in units of milligrams of solid material (colloids or particles) per litre of discharged condensate.

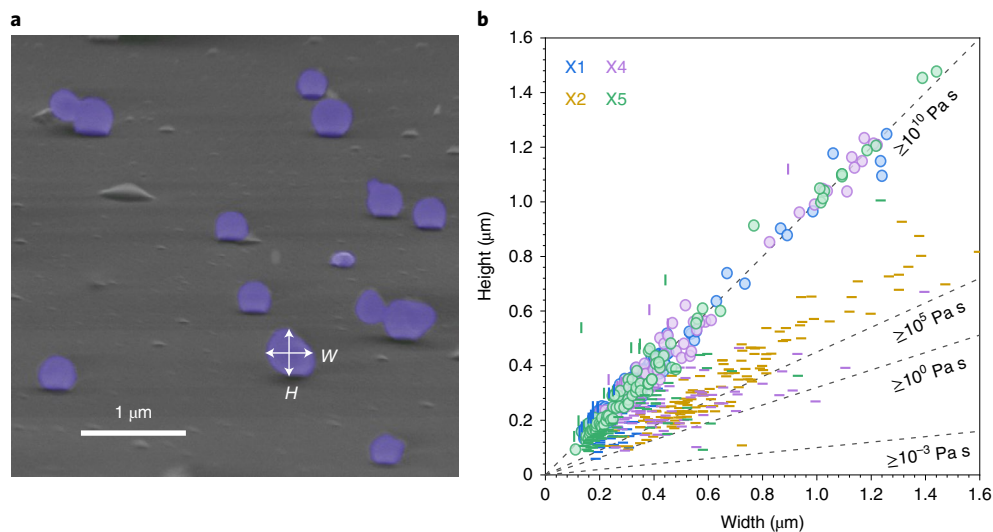


Fig. 3 | Size, morphology and viscosity characteristics of dry particles aerosolized from four samples of CIPP waste condensate. **a**, SEM image (in secondary electron mode) of particles imaged at a tilt angle of 75° , showing the particle morphology after impact on a substrate. Particles with high viscosity remain spherical after impact; liquid-like particles exhibit a flat morphology. H , height; W , width. **b**, Plot of particle height versus their width after impact,

referenced to particle standards of known viscosity (Supplementary Fig. 5). The viscosity characteristics of individual particles are inferred by comparison with the references (indicated by dashed lines). Circles correspond to spherical particles; vertical and horizontal line markers correspond to high-dome and flat particles, respectively.

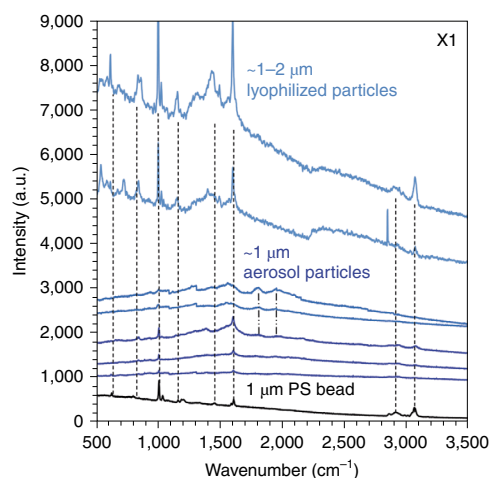


Fig. 4 | SERS spectra of individual dry EnvNP particles from the X1 sample of CIPP waste condensate. Representative SERS spectra of single particles from lyophilized residue (top two spectra) and individual dry airborne particles collected on a substrate. The dashed lines show the similarity between the spectral characteristics of a subset of particles and a standard PS microbead as reference. The apparent PS spectral features^{16,17} are as follows: stretching modes of aliphatic C–H at 2,931 cm^{-1} (asym.) and 2,868 cm^{-1} (sym.), stretching of aromatic C–H at 3,075 cm^{-1} and bending at 1,435 and 1,154 cm^{-1} , C=C vibration at 1,602 cm^{-1} , ‘breathing mode’ of the aromatic ring at 1,000 cm^{-1} , the combination band of the CH out-of-plane bending modes from the ring and the CH₂ rocking modes from the backbone at 852 cm^{-1} and C–C vibration at 614 cm^{-1} . The dashed-dotted lines indicate additional spectral characteristics specific to poly(styrene maleic anhydride)³¹, corresponding to C=O stretching at 1,889 and 1,807 cm^{-1} , observed in some of the particles. a.u., arbitrary units.

of these particles as EnvNPs. Furthermore, the vibrational spectra of individual particles recorded by surface-enhanced Raman spectroscopy (SERS) show the spectroscopic features of common microplastic materials (Supplementary Note 8). Figure 4 shows selected SERS spectra of relatively large ($>1 \mu\text{m}$) dry particles obtained from the waste condensates. These EnvNPs are likely polymers, with characteristic features in the 3,000 cm^{-1} region. In particular, polystyrene (PS) resonances are evident in the spectra of some of the particles, revealed by comparison with a PS microbead standard. Furthermore, particles exhibiting SERS signatures of other polymer materials, such as poly(styrene maleic anhydride) and polydimethylsiloxane, are also noteworthy (Supplementary Fig. 6)^{30,31}. The top two SERS spectra in Fig. 4 were recorded for $\sim 2 \mu\text{m}$ particles from lyophilized waste analyte from the X1 sample. These spectra show features similar to the PS standard. However, because of only minute quantities and the chemical complexity of the analytes in EnvNP particles, the features are relatively broad and have very low intensities, which renders their analysis difficult. Moreover, the detection limit of SERS for organic particles is $\sim 1 \mu\text{m}$, which hinders the detection of submicrometre EnvNPs. The spectral data shown in Fig. 4 and Supplementary Fig. 6 demonstrate the need to identify the composition of dry EnvNPs from CIPP emissions at scales finer than those accessible by SERS.

Synchrotron-based scanning transmission X-ray microscopy (STXM) enables the imaging of carbon speciation, allowing differentiation between different polymers distributed within internal particle structures with a lateral resolution of $\sim 35 \text{nm}$. Particle-specific ratios of the total carbon absorption to the particle diameter derived from STXM measurements were used to distinguish solid spherical EnvNPs from flat, domed particles having lower viscosity (Supplementary Note 10). Figure 5a shows the STXM images of selected solid EnvNP particles and their associated near-edge X-ray absorption fine structure (NEXAFS) spectra acquired at their carbon K-edge energy. The NEXAFS spectra

of the EnvNP particles share similar characteristics with reported thin-film polymer standards³² (Supplementary Note 10), with differences arising due to their multicomponent composition. Because of the chemical complexity of the emissions discharged from CIPP installations, the NEXAFS spectra of the investigated EnvNP samples are best interpreted as a mixture of multiple polymers. The systematic differences between the NEXAFS spectra of the solid particles identified in the aerosolized samples generated from the four waste condensates indicate that the chemical composition of the EnvNPs varies substantially between worksites where different operating conditions are employed. Figure 5b shows the composition maps of individual solid particles generated in our experiments, indicating that their interiors are dominated by organic components. Unlike the typical particles of urban photochemical smog, where the components of secondary organic aerosol tend to coat the inorganic and black carbon inclusions from primary emissions³³, the particles reported here show either organic-only composition or an inverted morphology of organic cores coated with inorganic components. This inverted morphology is consistent with the assumption that organic cores originate from the insoluble organic colloids present in the discharged waste condensate and are coated with thin layers of inorganic salts (probably carbonates) formed by precipitation as the microdroplets of wet aerosol dry out. It is also expected that additional organic solid particles may be formed by the condensation of soluble organic components that have polymerized in drying microdroplets. A quantitative assessment of organic volume fractions (OVFs) in individual particles by X-ray spectromicroscopy (Fig. 5c,d and Supplementary Note 10) showed overall minor contributions of inorganic salts in the observed particles. It is suggested that lateral chemical heterogeneity and the physical states of the atmospheric EnvNP particles from CIPP operations are likely influenced by both the resin material and specific curing conditions. Therefore, documenting the mass loading, composition and size of individual EnvNP particles collected at worksites and in systematic laboratory tests of CIPP emissions will allow source apportionment of this type of particle in real-world urban environments, prediction of their physical properties and evolution upon atmospheric ageing.

The deposits of white powder commonly observed on trees and other surfaces next to CIPP installation sites (Supplementary Note 12) are likely to be micro- and nanoplastic particles emitted during the process¹⁷. While it may be surprising that EnvNP particles have not been explicitly reported in the assessments of CIPP emissions and in more general studies characterizing the urban aerosol, there are compelling reasons for their lack of observation. EnvNP particles are resistant to decomposition on heating up to 400 °C observed in high-resolution transmission electron microscopy (HRTEM) experiments (Supplementary Note 11), suggesting that in situ particle analysis using thermoanalytical methods is unsuitable for their detection. Thus, if EnvNP particles were present in urban environments, common thermal desorption-based aerosol mass spectrometers would underestimate the organic particle concentration. Laser ablation single-particle mass spectrometry would detect EnvNP particles. However, extensive fragmentation of organic analyte on ablation would make it difficult to distinguish EnvNPs from other organic particles. Due to their solid, spherical morphology and polymer composition, off-line spectromicroscopy methods are likely to be advantageous for the detection and characterization of fine EnvNPs³³.

Public records indicate that 61–454 tonnes of resin are used for each CIPP project in US urban areas, where multiple sewer pipes are typically repaired (Supplementary Note 13)¹⁶. Laboratory studies show that, during the CIPP process, $\sim 9 \text{wt}\%$ of the organic resin material is discharged into the air¹⁶, which translates into $>5 \text{ tons}$ of organic chemical waste released into atmospheric and aquatic environments as gas- and condensed-phase emissions for each CIPP project^{12,14,16,17,34,35}. Based on a conservative estimate that the mass fraction of EnvNP particles is only $\sim 5\%$ of the total organic waste

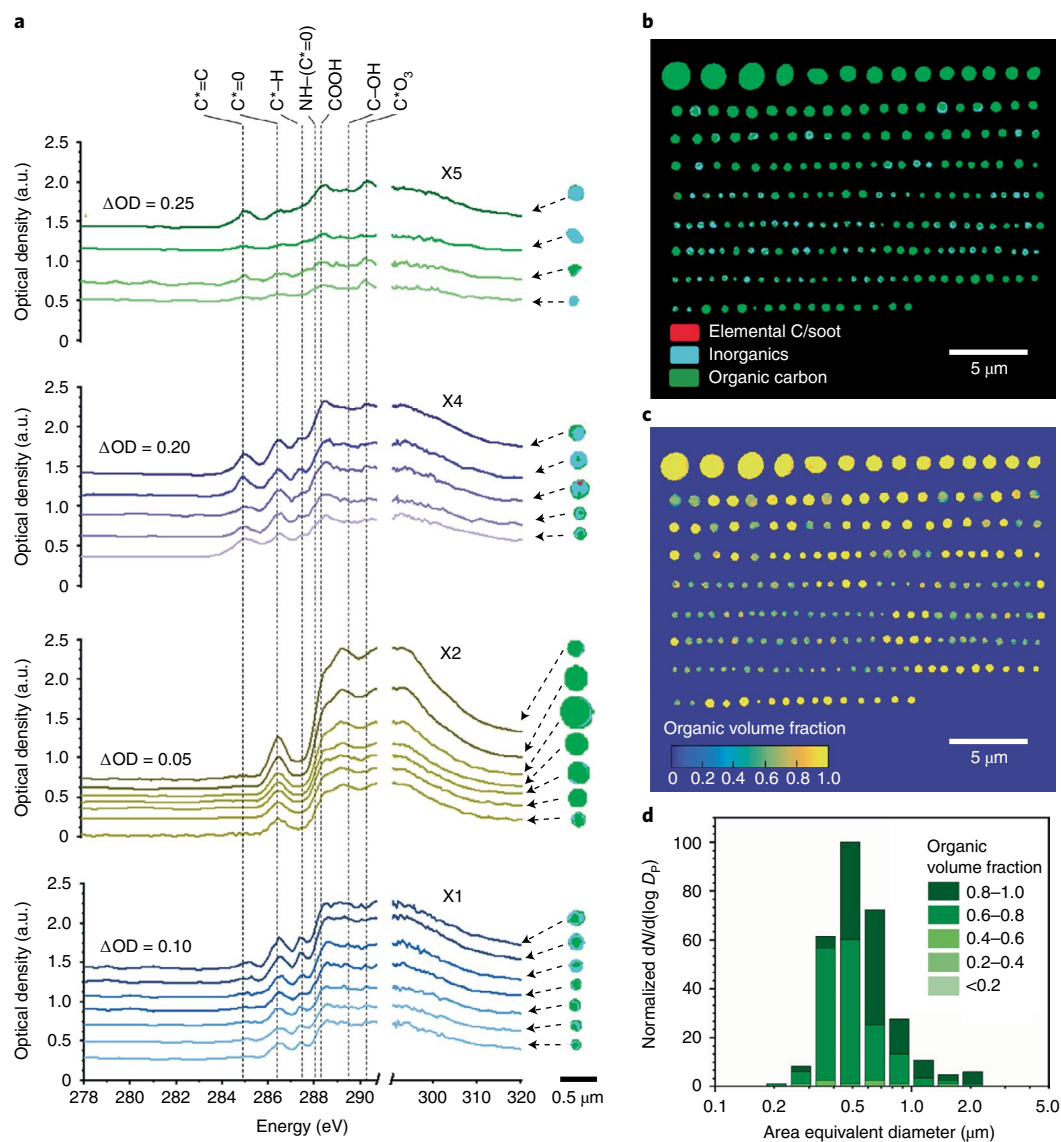


Fig. 5 | Carbon chemical bonding and mixing states of the EnvNPs from CIPP waste condensates. **a**, Carbon K-edge NEXAFS spectra of representative individual solid EnvNP particles from the four samples X1, X2, X4 and X5 (left). The corresponding individual particle maps show the organic carbon (green), black carbon (red) and inorganic (blue) content, which overlap for some particles (right). For each of the sample groups, the spectra are offset by incremental optical density (ΔOD) values, indicated in the legends. The dashed lines indicate the absorption of various carbon-containing groups. The characteristic peaks of X1 at 286.7 eV ($C^*=O$), 287.7 eV (C^*-H) and 288.5 eV (COOH) coincide with the peak positions of poly(acrylonitrile) and poly(vinyl alcohol) materials¹⁸. The single dominant spectral feature of X2 at 286.7 eV ($C^*=O$) is indicative

of poly(vinyl methyl ketone), widely used in industry as a crosslinked film¹⁸. Samples X4 and X5 show similar NEXAFS features at 284.9 eV ($C^*=C$), 286.7 eV ($C^*=O$), 287.7 eV (C^*-H), 288.5 eV (COOH) and 290.4 eV (C^*O_3), which align with poly(α -methylstyrene), polyether ether ketone and polystyrene (Supplementary Note 9). * denotes the $1s \rightarrow \sigma^*$ transitions. **b**, STXM composition maps for all samples indicate particles dominated by organic carbon. **c**, OVf maps of the same particles derived from quantitative analysis of the NEXAFS spectra of the particles. **d**, Histogram of the OVf values determined for individual particles plotted as a function of particle size show only minor contributions from inorganic components.

(Supplementary Table 1), their emission will be >0.25 tons per project. This scale of urban pollution is not well documented. In fact, it may eclipse many other common sources of pollution in urban areas. Many recent studies have shown that emissions from CIPP technology pose serious health risks to workers and the nearby public^{17,36,37}. Their results have led to US federal^{38,39}, California and Florida state^{40,41}, and industry actions, acknowledging the critical need to mitigate CIPP emissions due to human health effects and environmental impacts. However, all studies conducted so far have been limited to gas-phase and water-soluble chemical emissions, while emissions of EnvNP particles have not been considered.

Therefore there is an urgent need to quantitatively characterize the emissions of EnvNPs produced during CIPP manufacture as their environmental discharge and human exposure continue to occur. At present, little is known about which specific manufacturing conditions can be altered to reduce the emissions of EnvNPs and other pollutants. To provide evidence-based practical solutions for safer (less polluting) CIPP operation, systematic studies are needed to investigate how changing the resin, curing temperature, heating time, steam and other ingredient levels may affect the magnitude and composition of CIPP emissions, and to compare these with future field measurements.

Online content

Any methods, additional references, Nature Research reporting summaries, source data, extended data, supplementary information, acknowledgements, peer review information; details of author contributions and competing interests; and statements of data and code availability are available at <https://doi.org/10.1038/s41565-022-01219-9>.

References

- Schirinzi, G. F. et al. Cytotoxic effects of commonly used nanomaterials and microplastics on cerebral and epithelial human cells. *Environ. Res.* **159**, 579–587 (2017).
- Prata, J. C., da Costa, J. P., Lopes, I., Duarte, A. C. & Rocha-Santos, T. Environmental exposure to microplastics: an overview on possible human health effects. *Sci. Total Environ.* **702**, 134455 (2020).
- Lehner, R., Weder, C., Petri-Fink, A. & Rothen-Rutishauser, B. Emergence of nanoplastic in the environment and possible impact on human health. *Environ. Sci. Technol.* **53**, 1748–1765 (2019).
- Gigault, J. et al. Nanoplastics are neither microplastics nor engineered nanoparticles. *Nat. Nanotechnol.* **16**, 501–507 (2021).
- Cured-In-Place Pipe (CIPP) Market Size, Share, Trend, Forecast, and Competitive Analysis: 2020–2025. Report No. SRCE108; 1–273 (Stratview Research, 2019).
- Peng, J., Wang, J. & Cai, L. Current understanding of microplastics in the environment: occurrence, fate, risks, and what we should do. *Integr. Environ. Assess. Manag.* **13**, 476–482 (2017).
- Bucci, K., Tulio, M. & Rochman, C. M. What is known and unknown about the effects of plastic pollution: a meta-analysis and systematic review. *Ecol. Appl.* <https://doi.org/10.1002/eap.2044> (2020).
- Akdogan, Z. & Guven, B. Microplastics in the environment: a critical review of current understanding and identification of future research needs. *Environ. Pollut.* **254**, 113011 (2019).
- Wu, P. et al. Environmental occurrences, fate, and impacts of microplastics. *Ecotoxicol. Environ. Saf.* **184**, 109612 (2019).
- Wlasits, P. J., Stoellner, A., Lattner, G., Maggauer, K. & Winkler, P. M. Size characterization and detection of aerosolized nanoplastics originating from evaporated thermoplastics. *Aerosol Sci. Technol.* **56**, 176–185 (2022).
- Chen, G., Feng, Q. & Wang, J. Mini-review of microplastics in the atmosphere and their risks to humans. *Sci. Total Environ.* **703**, 135504 (2020).
- Ra, K. et al. Considerations for emission monitoring and liner analysis of thermally manufactured sewer cured-in-place-pipes (CIPP). *J. Hazard. Mater.* **371**, 540–549 (2019).
- Noh, Y. et al. Emergency responder and public health considerations for plastic sewer lining chemical waste exposures in indoor environments. *J. Hazard. Mater.* **422**, 126832 (2022).
- Matthews, E., Matthews, J. & Eklund, S. NASSCO CIPP Emissions Phase 2: Evaluation of Air Emissions from Polyester Resin CIPP with Steam Cure. Final Report (NASSCO, 2020).
- Hong, Z. et al. Characteristics of atmospheric volatile organic compounds (VOCs) at a mountainous forest site and two urban sites in the southeast of China. *Sci. Total Environ.* **657**, 1491–1500 (2019).
- Teimouri Sendesi, S. M. et al. An emerging mobile air pollution source: outdoor plastic liner manufacturing sites discharge VOCs into urban and rural areas. *Environ. Sci. Process. Impacts* **22**, 1828–1841 (2020).
- Teimouri Sendesi, S. M. et al. Worksite chemical air emissions and worker exposure during sanitary sewer and stormwater pipe rehabilitation using cured-in-place-pipe (CIPP). *Environ. Sci. Technol. Lett.* **4**, 325–333 (2017).
- Hinds, W. C. in *Aerosol Technology: Properties, Behavior, and Measurement of Airborne Particles* 46–48 (Wiley, 1999).
- Initial list of hazardous air pollutants with modifications (United States Environmental Protection Agency, 2022). <https://www.epa.gov/haps/initial-list-hazardous-air-pollutants-modifications>
- NSCEP. *An Exposure and Risk Assessment for Benzo[a]pyrene and Other Polycyclic Aromatic Hydrocarbons*. Report No. EPA-44074-85-020 (NSCEP, 1982).
- Foster, P. M., Mylchreest, E., Gaido, K. W. & Sar, M. Effects of phthalate esters on the developing reproductive tract of male rats. *Hum. Reprod. Update* **7**, 231–235 (2001).
- Lee, A. K. Y. et al. Formation of light absorbing organo-nitrogen species from evaporation of droplets containing glyoxal and ammonium sulfate. *Environ. Sci. Technol.* **47**, 12819–12826 (2013).
- Ortiz-Montalvo, D. L., Schwier, A. N., Lim, Y. B., McNeill, V. F. & Turpin, B. J. Volatility of methylglyoxal cloud SOA formed through OH radical oxidation and droplet evaporation. *Atmos. Environ.* **130**, 145–152 (2016).
- Bain, R. M., Pulliam, C. J., Thery, F. & Cooks, R. G. Accelerated chemical reactions and organic synthesis in Leidenfrost droplets. *Angew. Chem. Int. Ed.* **55**, 10478–10482 (2016).
- Petters, S. S. et al. Volatility change during droplet evaporation of pyruvic acid. *ACS Earth Space Chem.* **4**, 741–749 (2020).
- Nguyen, T. B. et al. Formation of nitrogen-and sulfur-containing light-absorbing compounds accelerated by evaporation of water from secondary organic aerosols. *J. Geophys. Res.: Atmos.* **117**, D01207 (2012).
- Marsh, B. M., Iyer, K. & Cooks, R. G. Reaction acceleration in electrospray droplets: size, distance, and surfactant effects. *J. Am. Soc. Mass. Spectrom.* **30**, 2022–2030 (2019).
- Laskin, J. et al. Molecular selectivity of brown carbon chromophores. *Environ. Sci. Technol.* **48**, 12047–12055 (2014).
- Reid, J. P. et al. The viscosity of atmospherically relevant organic particles. *Nat. Commun.* **9**, 956 (2018).
- Zhou, X.-X., Liu, R., Hao, L.-T. & Liu, J.-F. Identification of polystyrene nanoplastics using surface enhanced Raman spectroscopy. *Talanta* **221**, 121552 (2021).
- Schoukens, G., Martins, J. & Samyn, P. Insights in the molecular structure of low- and high-molecular weight poly(styrene-maleic anhydride) from vibrational and resonance spectroscopy. *Polymer* **54**, 349–362 (2013).
- Dhez, O., Ade, H. & Urquhart, S. G. Calibrated NEXAFS spectra of some common polymers. *J. Electron Spectrosc. Relat. Phenom.* **128**, 85–96 (2003).
- Laskin, A., Moffet, R. C. & Gilles, M. K. Chemical imaging of atmospheric particles. *Acc. Chem. Res.* **52**, 3419–3431 (2019).
- Najafi, M. et al. *Evaluation of Potential Release of Organic Chemicals in the Steam Exhaust and Other Release Points During Pipe Rehabilitation Using the Trenchless Cured-In-Place Pipe (CIPP) Method* (NASSCO, 2018).
- Nuruddin, M. et al. Evaluation of the physical, chemical, mechanical, and thermal properties of steam-cured PET/polyester cured-in-place pipe. *J. Compos. Mater.* **53**, 2687–2699 (2019).
- Ra, K. et al. Critical review: surface water and stormwater quality impacts of cured-in-place pipe repairs. *J. Am. Water Works Assoc.* **110**, 15–32 (2018).
- Li, X. et al. Outdoor manufacture of UV-cured plastic linings for storm water culvert repair: chemical emissions and residual. *Environ. Pollut.* **245**, 1031–1040 (2019).
- US Occupational Safety and Health Administration *Citation and Notification of Penalty, Inspection Number 1274028*. Report No. O524200 (US Department of Labor, 2017).
- LeBouf, R. F. & Burns, D. A. *Health Hazard Evaluation Report: Evaluation of Exposures to Styrene During Ultraviolet Cured-in-Place-Pipe Installation*. Report No. 2018-0009–3334 (US

- National Institute of Occupational Safety and Health, Centers for Disease Control and Prevention, 2019).
40. *Cure-in-Place Pipe (CIPP): Additional Considerations for Municipalities* (California Department of Public Health, 2017).
 41. *CIPP Safety Alert* (California Department of Public Health, 2018).

Publisher's note Springer Nature remains neutral with regard to jurisdictional claims in published maps and institutional affiliations.

Springer Nature or its licensor holds exclusive rights to this article under a publishing agreement with the author(s) or other rightsholder(s); author self-archiving of the accepted manuscript version of this article is solely governed by the terms of such publishing agreement and applicable law.

© The Author(s), under exclusive licence to Springer Nature Limited 2022

Methods

Samples of CIPP waste condensates

Aqueous condensates of the exhaust emissions discharged during four CIPP installations in Sacramento, California were collected¹⁷. One CIPP was manufactured with a non-styrene, low-volatile organic resin, and three were manufactured with a styrene-based resin. Stainless-steel air-sampling manifolds were used at each site to capture and condense airborne emissions, collected in Pyrex bottles as detailed by Sendesi et al.¹⁷. The samples obtained were sealed and refrigerated at -20°C pending analysis. In this work the waste samples were aerosolized to evaluate the size distributions and mass loadings of plausible atmospheric particle emissions. The particles obtained were also analysed using chemical imaging techniques. Further analyses were conducted to determine the size distributions and mass loadings of the colloids present in the original bulk samples, and to characterize the major solvent-soluble organic components present in the bulk condensates and to estimate their volatility. Further details are included in Supplementary Notes 1 and 2.

Particle size distributions of colloids and particles

The colloidal material in the waste condensate samples was quantified by dynamic light scattering measurements using a Zetasizer Nano-S instrument (Malvern Panalytical). For quantitative data analysis, the dispersant was assumed to be water, and the optical properties and density of the colloidal material were assumed to be those of polystyrene. The difference between the total organic carbon and the dissolved organic carbon in the waste condensate samples was used to estimate the lower limit of mass loadings of the colloidal material. The particle size distributions of dry aerosolized particles were measured using a scanning mobility particle sizer interfaced with a condensation particle counter (TSI, models 3081 and 3776). The volumes of the condensate samples consumed in the aerosolization experiments were recorded and used to relate the measured mass concentrations and particle size distributions of airborne dry particles to the volume of the waste condensate. The quantitative measurements of colloids and dry airborne particles are presented here as milligrams of colloids (or dry airborne particles) per litre of waste condensate. Additional details of these experiments are included in Supplementary Notes 2–4.

Molecular characterization of waste condensates

The components of the waste condensates extracted in acetonitrile–dichloromethane–hexane (2:2:1, by volume) were separated by reversed-phase high-performance liquid chromatography (HPLC). The separated fractions were characterized by a photodiode array detector (PDA) and a high-resolution mass spectrometer (HRMS) interfaced with electrospray ionization and atmospheric pressure photochemical ionization sources to identify both polar and non-polar organic components⁴². Details of the HPLC–PDA–HRMS analysis are included in Supplementary Note 5.

Chemical imaging of particles

The dry particles from the aerosolization experiments deposited onto solid substrates were imaged by microscopies that revealed both the morphology and spectroscopically determined chemical composition. A SEM microscope was used to image particle samples at a tilt angle of 75° to distinguish between solid (spherical) and liquid-like (flattened) particles. Their viscosities were then inferred from the observed particle height-to-width ratios by comparison with standards of known viscosity. The size and elemental composition of large ensembles of $>2,000$ particles per sample were analysed by CCSEM–EDX, providing statistically significant data on the particle-type populations and their elemental compositions⁴³. Additional details of viscosity measurements by SEM and CCSEM–EDX particle analysis are included in Supplementary Notes 7 and 9.

The vibrational spectra of individual solid organic particles were recorded using SERS. At present, Raman spectral features are commonly used to identify environmental microplastic particles and apportion them to the most common polymer types⁴⁴. SERS was used for rapid screening of dry samples to identify the polymer characteristics of EnvNP particles. Specific details of the SERS analysis are included in Supplementary Note 8.

STXM–NEXAFS spectromicroscopy at the carbon K-edge energy was used to obtain information on the chemical bonding of carbon within individual particles at a lateral resolution of ~ 35 nm, sufficient for a detailed analysis⁴⁵ of submicrometre EnvNP particles. Particle component maps⁴⁶ were constructed on the basis of NEXAFS spectral features indicative of carbon-specific functional groups and chemical bonding. Combined, the CCSEM–EDX and STXM–NEXAFS datasets allowed the grouping and assessment of EnvNP particle types and their representative mixing states. Additional details of the STXM–NEXAFS analysis are included in Supplementary Note 10.

Data availability

The datasets generated and analysed in this work are available for download as a zip file from <https://doi.org/10.4231/XR71-ZM27>. Datasets are provided for Figs. 2–5 and Supplementary Figs. 3, 5 and 7–10. Supplementary information is available in the online version of the paper. Correspondence and requests for materials should be addressed to A.L.

References

- Lin, P., Fleming, L. T., Nizkorodov, S. A., Laskin, J. & Laskin, A. Comprehensive molecular characterization of atmospheric brown carbon by high resolution mass spectrometry with electrospray and atmospheric pressure photoionization. *Anal. Chem.* **90**, 12493–12502 (2018).
- Laskin, A., Cowin, J. P. & Iedema, M. J. Analysis of individual environmental particles using modern methods of electron microscopy and X-ray microanalysis. *J. Electron Spectrosc. Relat. Phenom.* **150**, 260–274 (2006).
- Anger, P. M. et al. Raman microspectroscopy as a tool for microplastic particle analysis. *Trends Anal. Chem.* **109**, 214–226 (2018).
- Moffet, R. C., Tivanski, A. V. & Gilles, M. K. in *Fundamentals and Applications in Aerosol Spectroscopy* (eds Signorell, R. & Reid, J. P.) Ch. 17 (Taylor and Francis, 2010).
- Moffet, R. C., Henn, T., Laskin, A. & Gilles, M. K. Automated chemical analysis of internally mixed aerosol particles using X-ray spectromicroscopy at the carbon K-edge. *Anal. Chem.* **82**, 7906–7914 (2010).

Acknowledgements

This work was supported by the US National Science Foundation (grant nos. CBET-1624183 and CBET-2129166 (A.J.W. group), and CBET-2107946 (A.L. group)), the National Science Foundation Graduate Research Fellowship Program (grant no. DGE-1333468 (A.C.M.)) and the Purdue University Ross Fellowship program (B.N.P., S.A.L.S. and Y.N.). Any opinions, findings and conclusions or recommendations expressed in this material are those of the author(s) and do not necessarily reflect the views of the National Science Foundation. The CCSEM–EDX, HRTEM and SERS analyses, with guidance from N. Lata and Z. Cheng, were performed at the Environmental Molecular Sciences Laboratory, a National Scientific User Facility sponsored by OBER at PNNL. PNNL is operated by the US Department of Energy by the Battelle Memorial Institute under contract DE-AC06-76RLO. STXM–NEXAFS analyses were performed at beamline 5.3.2 of the Advanced Light Source at Lawrence Berkeley National Laboratory (LBNL), with guidance from D. Kilcoyne, M. Marcus and D. Shapiro. LBNL is supported by the Director, Office

of Science, Office of Basic Energy Sciences of the US Department of Energy under contract DE-AC02-05CH11231. STXM maps of particles were also acquired at the Canadian Light Source (CLS), with guidance from J. Wang. CLS is supported by the Canada Foundation for Innovation, Natural Sciences and Engineering Research Council of Canada, the University of Saskatchewan, the Government of Saskatchewan, Western Economic Diversification Canada, the National Research Council Canada and the Canadian Institutes of Health Research.

Author contributions

A.C.M., J.M.T. and A.L. conceptualized the framework, experiments and analytical methodologies of the study. Y.N., S.M.T.S., B.E.B., J.A.H. and A.J.W. conducted field studies and provided samples of the CIPP waste condensates. A.C.M., C.P.W. and B.N.P. performed the HPLC–HRMS measurements and analysed the data. J.M.T. and F.A.R.-A. analysed individual particles using SEM and STXM. S.A.L.S. performed the TEM analysis of heated particles. S.C. assisted with SEM experiments and R.C.M. assisted with STXM experiments and instrument operation. B.T.O.C. and P.Z.E.-K. performed the SERS analysis. A.C.M. and A.L. integrated the experimental datasets and wrote the manuscript, and all authors contributed its review and editing. A.J.W. and A.L. secured grant support for this study and managed the project.

Competing interests

A.J.W., J.A.H., B.E.B. and S.M.T.S. are named in a patent application (PCT application no. PCT/US18/28173) filed 18 April 2018 by the Purdue Research Foundation. The patent application pertains to the technologies for capturing CIPP waste condensates investigated in this study. The invention was developed with support from the US National Science Foundation (grant CBET-1624183). The remaining authors declare no competing interests.

Additional information

Supplementary information The online version contains supplementary material available at <https://doi.org/10.1038/s41565-022-01219-9>.

Correspondence and requests for materials should be addressed to Alexander Laskin.

Peer review information *Nature Nanotechnology* thanks the anonymous reviewers for their contribution to the peer review of this work.

Reprints and permissions information is available at www.nature.com/reprints.